Check for updates

Chemistry–A European Journal

Research Article
doi.org/10.1002/chem.202203501

Chemistry Europe
European Chemical Societies Publishing

www.chemeurj.org



The First Alkaline-Earth Azidoaurate(III), $Ba[Au(N_3)_4]_2 \cdot 4H_2O$

Yaprak Subaşı,[c] Elif Sena Tekin,[c] Yurii Prots,[a] Franziska Jach,[a, d, e] Mehmet Somer,[c] Semih Afyon,*[b] and Peter Höhn*[a]

Abstract: Transparent, dark orange $Ba[Au(N_3)_4]_2 \cdot 4H_2O$ was synthesized by reaction of $Ba(N_3)_2$ and $AuCl_3$ or $HAuCl_4$ in aqueous solution. The novel barium tetraazidoaurate(III) tetrahydrate crystallizes in the monoclinic space group *Cc* (no. 9) with $a = 1813.68(17)$ pm, $b = 1737.95(11)$ pm, $c = 682.04(8)$ pm and $\beta = 108.849(4)°$. The predominant structural features of $Ba[Au(N_3)_4]_2 \cdot 4H_2O$ are two crystallographically independent discrete anions $[Au(N_3)_4]^-$ with gold in a tetragonal planar coordination by nitrogen. Vibrational spectra show good agreement with those of other azidoaurates(III). Upon drying, this salt was shown to be a highly explosive material.

Introduction

Inorganic azides receive great attention due to their explosive nature, shock and friction sensitivity, as energetic materials, as well as starting materials for the synthesis of both nitrides and nitridometalates.[1–4] Our recent interest into azidometalates was rekindled in testing them as a novel synthetic route towards nitridoaurates and gold nitrides.

The binary azides of alkali metals such as LiN_3, NaN_3, KN_3, RbN_3 and CsN_3,[5–6] like the heavy alkaline-earth metal azides $AE(N_3)_2$ (AE = Ca, Sr, Ba),[7–9] contain linear and (nearly) symmetrical azide species. In these phases, the coordination numbers of cations by azide range from six (LiN_3)[6] to eight (KN_3,[10] $Sr(N_3)_2$)[11,12] and nine ($Ba(N_3)_2$).[11,13,14]

Binary gold azides are hitherto unknown. First reports dating to 1898[15] were shown to be in reality ternary sodium azidoaurate(III) in 1957.[16] The crystal structures and vibrational spectroscopic properties as well as topology and bonding of ternary azidoaurates(III) $A[Au(N_3)_4]$ with monovalent metal ions (A = K, Rb, Cs)[17] or complex cations ($A = [As(C_6H_5)_4]$)[18] have been investigated in more detail. The explosive nature of the azidoaurates has been shown to increase with decreasing cationic radius.[19] All azidoaurate(III) anions $[Au(N_3)_4]^-$ known up to now feature square-planar coordination of Au by N with azide species displaying a N–N–N bond angle of $172 \pm 3°$ and two different N–N bond lengths;[20] however, they show structural variety besides the ubiquitous "windmill".

Although binary azides of the alkaline-earth elements were extensively investigated,[4] the only multinary azides containing both alkaline-earth and transition metals reported up to now are the cluster compounds $AE_2[Nb_6(N_3)_6Cl_{12}] \cdot 4H_2O$ (AE = Ca, Sr)[21] and the nitridometalates $Ba_9[MN_4]_2(N_3)N$ (M = Nb, Ta).[22–23] However, the latter ones were later proven to be carbodiimide-oxides $Ba_9[MN_4]_2(CN_2)O$.[24]

In this study, we present the first alkaline-earth gold azide $Ba[Au(N_3)_4]_2 \cdot 4H_2O$, which was synthesized in a two-step reaction. The binary azide $Ba(N_3)_2$ was prepared through a column ion-exchange method. Single crystals of the new phase $Ba[Au(N_3)_4]_2 \cdot 4H_2O$ are obtained in a second step through the reaction of $Ba(N_3)_2$ with either $AuCl_3$ or $HAuCl_4$. The crystal structure and vibrational spectroscopic properties are reported in detail.

Explicit Safety Hazard! Barium tetraazidoaurate(III) tetrahydrate, $Ba[Au(N_3)_4]_2 \cdot 4H_2O$, exploded on various occasions and is an extremely dangerous material. All experiments to obtain samples free of crystal water resulted in even more sensitive materials and ended in heavy explosions.

Results and Discussion

Crystal structure

The barium azidoaurate(III) $Ba[Au(N_3)_4]_2 \cdot 4H_2O$ ***A*** (Figure 1) crystallizes in the non-centrosymmetric monoclinic space group *Cc* (No. 9, $a = 1813.68(17)$ pm, $b = 1737.95(11)$ pm, $c = 682.04(8)$ pm, $\beta = 108.849(4)°$). Table 1 and Table S1 in the

[a] Dr. Yu. Prots, Dr. F. Jach, Dr. P. Höhn
Chemische Metallkunde
Max-Planck-Institut für Chemische Physik fester Stoffe
01187 Dresden (Germany)
E-mail: hoehn@cpfs.mpg.de

[b] Asst. Prof. Dr. S. Afyon
Energy Technologies Institute
Gebze Technical University
41400 Gebze/Kocaeli (Turkey)
E-mail: safyon@gtu.edu.tr

[c] Y. Subaşı, E. S. Tekin, Prof. Dr. M. Somer
Department of Chemistry, Koç University
Rumelifeneri Yolu, 34450 Sarıyer, Istanbul (Turkey)

[d] Dr. F. Jach
Faculty of Chemistry and Food Chemistry
Technische Universität Dresden
01062 Dresden (Germany)

[e] Dr. F. Jach
Fraunhofer Institute for Integrated Systems and Device
Technology IISB
Schottkystraße 10, 91058 Erlangen (Germany)

Supporting information for this article is available on the WWW under https://doi.org/10.1002/chem.202203501

© 2022 The Authors. Chemistry - A European Journal published by Wiley-VCH GmbH. This is an open access article under the terms of the Creative Commons Attribution License, which permits use, distribution and reproduction in any medium, provided the original work is properly cited.

© 2022 The Authors. Chemistry - A European Journal published by Wiley-VCH GmbH

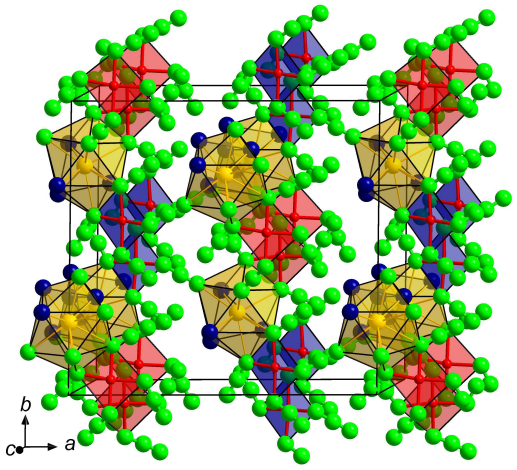


Figure 1. Crystal structure of $Ba[Au(N_3)_4]_2 \cdot 4H_2O$ (Ba: yellow, Au: red, N: green, O: blue). Complex anions $[Au(N_3)_4]^-$ (**Au1**: red, **Au2**: blue) as well as coordination polyhedra around Ba (yellow) are emphasized.

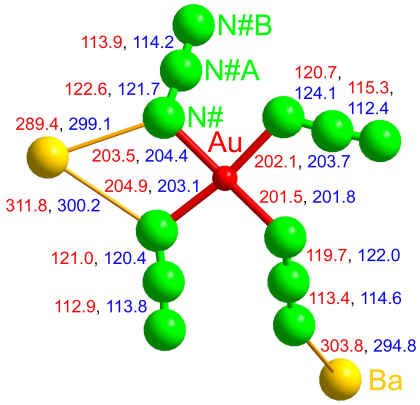


Figure 2. The complex azidoaurate anions and their Ba coordination in the crystal structure of $Ba[Au(N_3)_4]_2 \cdot 4H_2O$. Color coded distances [pm] refer to complex anions **Au1** (red) and **Au2** (blue).

Table 1. Crystallographic data for $Ba[Au(N_3)_4]_2 \cdot 4H_2O$; more details are given in Table S1.

Composition	$Ba[Au(N_3)_4]_2 \cdot 4H_2O$
crystal color, shape	orange-brown transparent prism-like crystals
refinement method	single crystal, SHELXL-2018[25–26]
crystal system	monoclinic
space group	*Cc* (No. 9)
a [pm]	1813.68(17)
b [pm]	1737.95(11)
c [pm]	682.04(8)
β [°]	108.849(4)
V [10^6 pm]	2034.6(3)
Z	4
molar mass [$g \cdot mol^{-1}$]	939.58
no. refl. unique	5847
R_{int}	0.0513
refined parameters	280
*R*1, *wR*2 (all data)	0.040, 0.081

Supporting Information contain crystallographic and refinement data; positional and displacement parameters are given in Tables S2 and S3. Selected distances and angles are given in Figure 2 and Table S4. The H positions in ***A*** could not be localized and refined; the presence of hydrogen bonds as well as a potential split position of one azide ion is discussed in Tables S5–S7.

Although ***A*** may be formally considered as a pseudobinary phase $AB_2 \equiv (Ba(H_2O_4))_1[Au(N_3)_4]_2$, the centers of gravity of the constituents do not mimic any known simple prototype.

Predominant structural features in ***A*** are two symmetry-independent complex azidoaurate anions $[Au^{III}(N_3)_4]^-$ (**Au1**, **Au2**; Figure 2) of similar geometry. In both, the gold centre is located within a (slightly distorted) tetragonal planar coordination sphere built up by the inner N species of the azide ions. The Au–N distances within the complex anions (**Au1**: d_{ave} = 203.0 pm; **Au2**: d_{ave} = 203.2 pm) are in the range typical for azidoaurate(III) compounds ($[As(C_6H_5)_4][Au(N_3)_4]$: d = 203.2 pm;[27] $[Me_4N][Au(N_3)_4]$: d_{ave} = 202.5 pm;[28] $Cs[Au(N_3)_4]$: d_{ave} = 203.2 pm),[17] whereas in organic azido gold(I) compounds, the Au–N distances are significantly longer ($((C_6H_5)_3PAu^I[N_3]$: d = 210.0 pm).[18]

For all azide species in both azidoaurate anions (Figure 2), the angles Au#–N#–N#A are similar, ranging between 115.4(8)°–124.2(10)° (**Au1**) and 115.3(9)°–119.8(11)° (**Au2**), respectively.

As is usual in azidoaurates, the individual N–N bond lengths in the symmetry independent azide ions are clearly different with distances towards the gold contact N#–N#A (d_{ave}(**Au1**) = 121.0 pm, d_{ave}(**Au2**) = 122.0 pm) being significantly longer than the distance towards the terminal N atom (N#A≡N#B: d_{ave} (**Au1**) = 114.0 pm, d_{ave}(**Au2**) = 113.8 pm), but in the range observed in other azidoaurates ($Cs[Au(N_3)_4]$: d = 119.6/113.4 pm;[17] $[As(C_6H_5)_4][Au(N_3)_4]$: d = 121.2/113.6 pm).[27] In binary barium azide, the N–N distances in both nearly symmetric azide anions are 116.7–118.0 pm;[11] the average N–N distance in ***A*** is within the same region (d_{ave} = 117.7 pm). The N–N–N angles in the azide ions (172.0(17)°–176.6(14)°) are slightly smaller than 180°, but in a range expected for non-centrosymmetric azides. Similar values of N–N–N angles down to 170° have been found for both azidoaurates ($Cs[Au(N_3)_4]$: 173.5(18)°/175.9(18)°;[17] $[As(C_6H_5)_4][Au(N_3)_4]$: 174.4°/175.8°)[27] and azides which are covalently bonded to a metal or an organic substituent.[29,30]

Whereas in both **Au1** and **Au2** the central AuN_4 unit is nearly planar, the dihedral angles between the azide groups and the AuN_4 plane vary between 0° and 40°, indicating significant torsion. The coordination spheres of the azide ions rather mimic uncharged complexes than inorganic ionic compounds. In both complex anions **Au1** and **Au2**, one azide group connects only to gold as its next-nearest neighbour, two connect to barium and gold through the same N species, and one connects to Au and Ba through opposite N species. By this, the coordination spheres of the azide ions are significantly different compared to $Ba(N_3)_2$,[11] in which the azide groups are surrounded by four and five barium atoms each, and $Ba(N_3)_2 \cdot H_2O$ (3 Ba in the coordination sphere),[31] respectively.

© 2022 The Authors. Chemistry - A European Journal published by Wiley-VCH GmbH

15213765, 2023, 11, Downloaded from https://chemistry-europe.onlinelibrary.wiley.com/doi/10.1002/chem.202203501 by Koc University, Wiley Online Library on [10/05/2023]. See the Terms and Conditions (https://onlinelibrary.wiley.com/terms-and-conditions) on Wiley Online Library for rules of use; OA articles are governed by the applicable Creative Commons License

Au–Au distances between neighboring anions are clearly different: d(Au1–Au1) = 387.3 pm, d(Au2–Au2) = 451.3 pm; however, both are significantly larger than the sum of the van der Waals radii (332 pm),[32] therefore ruling out any Au···Au interactions.

The complex anions **Au1** and **Au2** with C_1 symmetry establish a new conformation isomer in azidoaurate chemistry (Figure 3). Up to now, two different types of complex azidoaurate ions have been observed: in compounds with large cations, the azidoaurate ions show C_{4h} symmetry (e.g., $[As(C_6H_5)_4][Au(N_3)_4]$[18]), whereas in all alkali metal azidoaurates the complex anion has C_2 symmetry.[17,33] Similar and further topologies are also observed in selected azidopalladates(II)[19,34,35] and azidoplatinates(II).[35]

The coordination sphere of the barium cations (CN = 10) containing six azide groups of four different complex anions and four water molecules forms a highly irregular polyhedron (Figure 4). The Ba–N distances (d = 289.3(10)–311.9(13) pm, d_{ave} = 299.8 pm) are longer, whereas the Ba–O distances (d = 272.5(12)–289.2 (19) pm, d_{ave} = 279.2 pm) are shorter compared to $Ba(N_3)_2$ (d = 291.1 pm)[11] and $Ba(N_3)_2 \cdot H_2O$ (d(Ba–N) = 291.8 pm; d(Ba–O) = 291.5 pm);[36] however, in both latter azides the coordination number of the cation is only 9, and the water molecules coordinate to two Ba species.

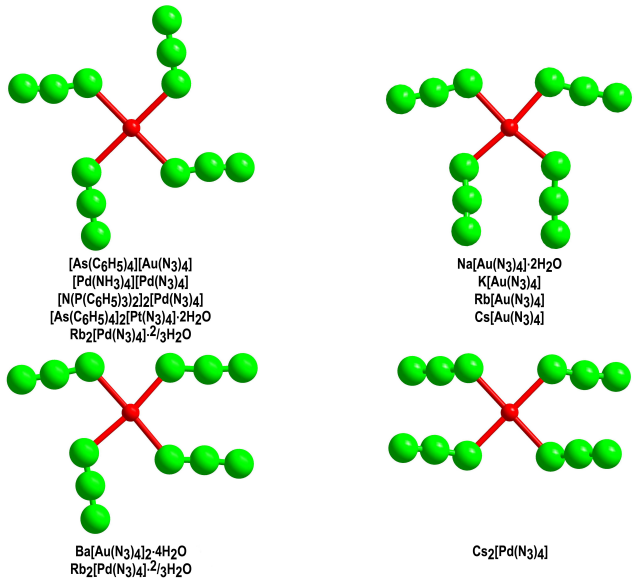


Figure 3. Azidometalate anions with square planar coordination of the central atom show a wide variety of conformations besides the ubiquitous windmill.

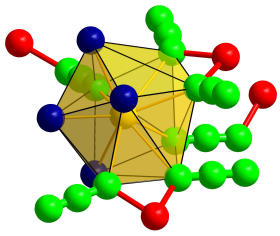


Figure 4. Detail of the Ba coordination sphere in $Ba[Au(N_3)_4]_2 \cdot 4H_2O$ (Ba: yellow, Au: red, N: green, O: blue). Water molecules coordinate to one Ba only; neighboring complex anions are indicated.

Vibrational spectroscopy

The vibrational spectra of tetraazidoaurate anion $[Au(N_3)_4]^-$ with monovalent metal ions or complex cations such as K, Rb and Cs or $[As(Phen)_4]$ have been already reported.[17,18] The title compound $Ba[Au(N_3)_4]_2 \cdot 4H_2O$ is the first example with a divalent counterion, Ba^{2+}.

The common spectroscopically relevant unit in metal tetraazidoaurates is the discrete $[Au(N_3)_4]^-$ moiety with the symmetry $C_{4h}/4/m$ (idealized case) for which a total of 33 vibrations are expected, distributed to 25 modes:

$$\Gamma_{vib}\ (C_{4h}) = 5\ A_g\ (RE) + 6\ B_g\ (RE) + 2\ E_g\ (RE)$$
$$+3\ A_u\ (IR) + 3\ B_u\ (-,-) + 6\ E_u\ (IR)$$

Hereby, the g species are only Raman and the u ones are only IR active. B_u is both inactive and forbidden. There are two crystallographically distinct gold atoms, which occupy the site $C_i/\bar{1}$. A vibrational analysis performed on the actual centrosymmetric point group C_i results in 33 fundamentals (15 A_g + 18 A_u) for which the rule of mutual exclusion still applies. We expect two types of band splitting/band multiplications:

1) The splitting of the double degenerate E_g and E_u modes by virtue of the site symmetry reduction and
2) The existence of two crystallographic different azidoaurate anions with slight but significantly different bond lengths and angles giving rise to two sets of internal modes varying only slightly in their wavenumbers.

There are four formula units in the unit cell and two distinct molecules in the primitive spectroscopic cell, so that a factor group splitting will not occur.

The Raman and infrared spectra of the title compound (Detail: Figure 5, total: Figure S3, Table S8) reveal great resemblance to those of their alkali metal homologues both in the band intensities and the position of the internal frequencies, but are more patterned due to above mentioned crystal field effects.[17]

Consequently, the vibrational spectra of $Ba[Au(N_3)_4]_2 \cdot 4H_2O$ can be interpreted on the idealized C_{4h} symmetry by regarding the C_i site symmetry and the presence of the two distinct azidoaurate units in the monoclinic unit cell.

Based on the vibrational data of the $A[Au(N_3)_4]$ (A = K, Rb, Cs, $[As(Phen)_4]$]) series,[17–18] the spectra can be divided into four well-separated wave regions: 1) ν(N–N≡N) stretches (2100–1000 cm^{-1}), 2) in and out of plane deformations δ(N–N≡N) and γ(N–N≡N) (750–500 cm^{-1}), 3) ν(Au–N) valence vibrations (around 400 cm^{-1}), and 4) δ(N–Au–N) and δ(Au–N–N) deformations, as well as τ(Au–N–N) and τ(N–N≡N) torsions (< 300 cm^{-1}). In addition, there are four high frequent peaks located between 3000–3600 cm^{-1} and a doublet around 1650 cm^{-1} indicating the presence of hydrate water. The

© 2022 The Authors. Chemistry - A European Journal published by Wiley-VCH GmbH

15213765, 2023, 11, Downloaded from https://chemistry-europe.onlinelibrary.wiley.com/doi/10.1002/chem.202203501 by Koc University, Wiley Online Library on [10/05/2023]. See the Terms and Conditions (https://onlinelibrary.wiley.com/terms-and-conditions) on Wiley Online Library for rules of use; OA articles are governed by the applicable Creative Commons License

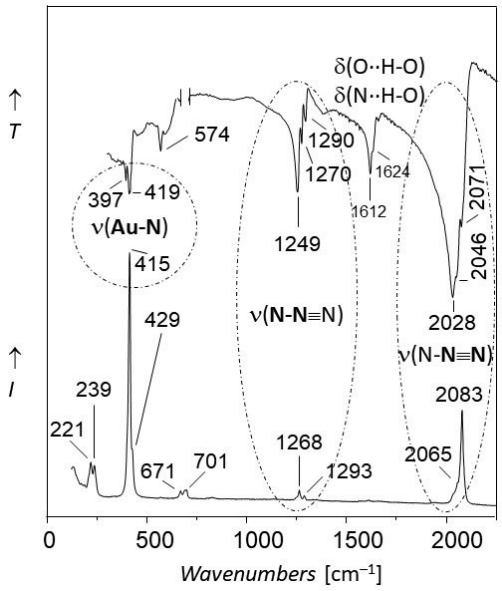


Figure 5. Vibrational spectra of $Ba[Au(N_3)_4]_2 \cdot 4H_2O$. Intensity (Raman) and transmission (IR-ATR) in arbitrary units, for experimental conditions, see text. The complete spectra are shown in Figure S3.

discussion of the hydrogen bonding modes will be conducted at the end of the section.

Similar to the afore-mentioned alkali metal azidoaurate series, the distribution of the bonding electrons within the terminal azide groups in $[Au(N_3)_4]^-$ is not symmetric, that is, the two outermost **N** atoms (–N–**N**≡**N**) form shorter bonds with increased bond order,[17] while the inner (–**N**–**N**≡N) bonds are significantly longer (Figure 2, Table S4). These findings are also reflected in the frequencies of the terminal azido groups. The weak Raman bands at 1268 and 1293 cm^{-1} and the medium strong IR absorption at 1249 cm^{-1} with the two shoulders at 1270 and 1290 cm^{-1} represent the ν(N–N) stretches of the longer inner bonds with respect to each other. The originally antisymmetric stretch of the free azide anion is now represented by the vibrations of the shorter outermost ν(N≡N) groups and are observed in Raman as a very strong peak at 2083 cm^{-1} with the shoulder at 2065 cm^{-1}. Their IR pendants are registered as the strong absorption at 2028 cm^{-1} with the shoulders at 2046 and 2071 cm^{-1}, respectively.

In-plane bending motions of the azido groups are recorded as weak bands at 720 cm^{-1} (IR) and 671 and 701 cm^{-1} (Raman). The assignment of the modes in the low frequency region (< 300 cm^{-1}) δ(N–Au–N), δ(Au–N–N) and τ(Au–N–N) bending and torsion modes are is depicted in Table S8.

Based on data reported previously, the gold-nitrogen stretching frequencies are expected around 400 cm^{-1}.[17] The symmetric (Au–N) modes were registered as the most intense band in the Raman spectrum at 415 cm^{-1} with a shoulder at 429 cm^{-1}. The corresponding antisymmetric valence modes (Au–N) are located as medium to weak absorptions at 419 and 397 cm^{-1}, respectively.

The overall comparison of observed wave numbers for the $[Au(N_3)_4]^-$ anions in $Ba[Au(N_3)_4]_2 \cdot 4H_2O$ harmonize very well with those reported for $K[Au(N_3)_4]$ and the coordination compound $[As(Ph)_4][Au(N_3)_4]$ given in Table S8.[17–18]

The comparison of the wavenumbers of stretching modes for the outermost (N≡N) and the inner (N–N) bonds shows a slight but significant shift to higher wavenumbers in favor of the Ba compound. These observation are in good accordance with previous reports[37,38] and can be explained by reduction of partial negative charge on the $[Au(N_3)_4]^-$ groups by the positive counterions which in turn will give rise to an increase of the (N–N) frequencies and force constants (counterion effect). The effect is more pronounced in presence of strong electropositive small cations with high positive charges. Thus, divalent Ba is expected to influence the (N–N) wavenumbers stronger than the monovalent alkali metals, which indeed is the case.

Due to the existence of the two sets of distinct tetraazidoaurate moieties in the unit cell with very similar structural parameters and wavenumbers, an exact assignment based on symmetry species (e.g., A_g, E_u, etc.) was practically impossible. More reasonable is, thus, the interpretation built on characteristic frequency regions as depicted in Figure 5.

The calculation of the force constants were carried out by the software program Prometheus 5.1[39] using averaged frequencies. As expected, the calculated (N–N) force constants with f(**N**–**N**) = 17.70 and 9.46 N cm^{-1} for the outermost and the inner (**N**–**N**) bonds, respectively, follow the same trend as the respective frequencies discussed above, being only slightly higher than those for the alkali homologues ($Cs[Au(N_3)_4]$: 15.44 Ncm^{-1}, 10.08 cm^{-1}).[17] Using these values and Siebert's equation for bond orders[40–41] one obtains for the (N–N) bond orders N = 2.57 (**N**≡**N**; outermost) and 1.42 (**N**–**N**; inner), respectively.

In summary, the vibrational spectra of $Ba[Au(N_3)_4]_2 \cdot 4H_2O$ are showing good agreement with those of the series $A[Au(N_3)_4]$ (A = K, Rb, Cs, $[As(Phen)_4]$) both in vibrational frequencies, as well as of for the (N–N) force constants and bond orders. The slight blue shift of the (N–N) stretchings with respect to the monovalent azidoaurates is due the counterion effect of the divalent Ba^{2+}.

Hydrate water and hydrogen bonding vibrations

The vibrational spectroscopic detection of the presence of hydrate water and hydrogen bonding occurs by the characteristic absorptions around 1550–1750 cm^{-1} and 3000–3500 cm^{-1}, representing δ(H–O–H) bendings and ν(O–H) stretches, respectively.[42] Thus, the broad IR peaks at 3309, 3456, 3531 and 3579 cm^{-1} and the band 1612 cm^{-1} with the shoulder at 1624 cm^{-1} are stemming from valence vibrations and deformations of hydrogen bonding of O···H···OH type. Due to the polarity of the O–H bond, water/hydrated water and hydrogen bonding peaks appear in Raman spectrum usually with low or very low intensities. Accordingly, the ν(O–H) stretch is registered as a very weak and broad Raman band at around 3520 cm^{-1}, while the OH bendings around 1600 cm^{-1} are completely absent (Figure 5). The next question which may

© 2022 The Authors. Chemistry - A European Journal published by Wiley-VCH GmbH

15213765, 2023, 11, Downloaded from https://chemistry-europe.onlinelibrary.wiley.com/doi/10.1002/chem.202203501 by Koc University, Wiley Online Library on [10/05/2023]. See the Terms and Conditions (https://onlinelibrary.wiley.com/terms-and-conditions) on Wiley Online Library for rules of use; OA articles are governed by the applicable Creative Commons License

arise in this context is whether there are any spectral hints for other type of hydrogen bonding involving the nitrogen atoms of the azide groups, such as N···H···O–H interactions. For this purpose, we have synthesized $Ba(N_3)_2 \cdot H_2O$[31] and measured the IR spectrum which shows beside the well-known azide peaks ($\nu 3 = 627$ (m), 647 (sh) cm^{-1}; $\nu 2 = 2032$ (sh), 2050 (vs) cm^{-1}) the expected hydrate modes at about 3360 (b, mw) and 1626 (w)/ 1652 (sh) cm^{-1}. The results underline that the nature of the hydrogen bonding in $Ba(N_3)_2 \cdot H_2O$ and $Ba[Au(N_3)_4]_2 \cdot 4H_2O$ are very similar, however, due to the higher hydrate water content the band intensities in the barium azidoaurate compound is significantly higher. Furthermore, the spectra allow no clear comment on the presence of hydrogen bonding other than that of H···OH type. This statement is made more difficult by the fact that (N···HO) and (H···OH) modes fall more or less in the same spectral range.[42]

Conclusions

The transparent orange compound $Ba[Au(N_3)_4]_2 \cdot 4H_2O$ crystallizes in the non-centrosymmetric space group *Cc*, containing two crystallographically different discrete anions with gold in planar coordination by nitrogen; the vibrational spectra were analyzed in detail based on the idealized point group C_{4h} of the spectroscopically relevant unit $[Au(N_3)_4]^-$. The azidoaurate anions show a new configuration and thus extend previous knowledge regarding square-planar coordinated azidometallates, especially concerning the closely related phases containing palladium.

Experimental Section

Synthesis: ***CAUTION!*** Due to the highly explosive nature of the title compounds, all handling was carried out under extreme safety conditions during experiments (protective shields, goggles and gloves) using minute amounts of samples. It is mandatory to wear protective gear and to prevent shock, heat, and intense radiation on samples.

Synthesis of $Ba(N_3)_2$: White solid NaN_3 (Merck, 99.9%, recrystallized in water) and H_2SO_4 were reactants to obtain HN_3 in an ion-exchange column. The anhydrous binary azide, $Ba(N_3)_2$, was synthesized by using the obtained HN_3 and the corresponding carbonate $BaCO_3$ (Alfa, 99.9%) by ion-exchange column method in water:

$$BaCO_3 + 2HN_3 \rightarrow Ba(N_3)_2 + H_2CO_3 \quad (1)$$

The resin column ($l = 775$ mm, $\varnothing_i = 14.2$ mm) was filled with acidic cation-exchange resin (DOWEX 50WX8-400), and ion-exchange was performed by using HN_3 with a 5 mL min^{-1} flow rate. The white product was collected after drying at 60 °C.

Synthesis of $Ba(N_3)_2 \cdot H_2O$:[31] 100 mg anhydrous barium azide salt was dissolved in 20 mL of distilled water, which was flushed free of CO_2 with Ar gas prior to use. On further purging with argon gas for 4–6 h through the clear solution, colorless column shaped crystals of $Ba(N_3)_2 \cdot H_2O$ started to precipitate. The crystallites maintain their transparency both in the mother liquid and shortly after removal, however, they became turbid on longer standing in air due to the loss of the hydrate water.

Synthesis of $Ba[Au(N_3)_4]_2 \cdot 4H_2O$: Treatment of $Ba(N_3)_2$ and $AuCl_3$ in molar ratio of 2.5:1 gave the best results. The starting materials, $Ba(N_3)_2$ (0.064 g/0.289 mmol) and $AuCl_3$ (0.035 g/0.115 mmol, Sigma–Aldrich, 99.99%), were dissolved in 2 mL water each; the solutions were reacted with a slight excess of alkaline-earth azide according to (2):

$$2\,AuCl_3 + 5\,Ba(N_3)_2 \rightarrow Ba[Au(N_3)_4]_2 + Ba(N_3)_2 + 3\,BaCl_2 \quad (2)$$

Upon combining, the color of the aquaeous solution instantaniosly changed to a deep orange. The obtained mixture was kept in in a large crystallizing dish for 12 to 60 h in a slightly cold environment (~5 °C) to obtain crystals of the title compound. After few days, large transparent orange-red crystalline agglomerates in form of brittle and often twinned needle-like plates were obtained upon evaporization of the solvent. They were highly explosive when dry, exposed to pressure, heat, or intense radiation, Most of the colorless by-products, presumabely unreacted $BaCl_2$, $Ba(N_3)_2$, and other phases, could be mechanically removed. Re-crystallization in ethanol or isopropanol not only removed the remaining traces of impurities, but also improved crystal quality. After the evaporation of the solution, translucent orange-red single crystals could be obtained, suitable to be examined by X-ray single crystal diffraction.

The use of $HAuCl_4$ (Sigma–Aldrich, 99.9%) instead of $AuCl_3$ gave similar results. Temperature treatment experiments were performed using either a hot plate or an ice bath in the range of 273–323 K without improving results. Due to the highly explosive nature of the title compound, the content of N and O in the bulk material could not be determined quantitatively by carrier gas hot-extraction technique. In preliminary experiments with sample amounts below 1 mg, heavy explosions threatened to damage not only the crucibles used for the analysis, but also the analyser itself. All experiments to remove crystal water, either by slow heating or by cautious evacuation, resulted directly in explosions, or even more sensitive, dark red and optically amorphous materials were obtained. The slightest touch or just handling sample holders loaded with these substances led to heavy explosions. Analysis of presumably water-free specimen was therefore impossible.

X-ray diffraction: Single crystals of the title compound, which were suitably sized for X-ray single crystal diffraction, were glued to the tips of glass fibres. Intensity data collection was performed at room temperature on a Rigaku AFC7 automatic diffractometer equipped with a Saturn 724+CCD detector with MoKα radiation using a graphite-monochromator and the ϕ oscillation scan technique. The crystal structure of the title compound was solved using SHELXS-2018 and refined using the full-matrix least-squares procedure with the SHELXL-2018 software package, see Tables 1 and S1–S3 for details.[25–26] It was not possible to localize and refine hydrogen positions. The highest peaks in the residual electron density map are located roughly centered between Au1, N11, and N11A and between Au2, N22 and N22A and have no structural significance.

The result of the refinement suggested the description of a nitrogen position as a split position. A corresponding refinement (Tables S1, S5, and S6) was carried out, but the result shows no significant improvement and does not affect the description of the crystal structure.

Deposition Number 2218579 contains the supplementary crystallographic data for this paper. These data are provided free of charge by the joint Cambridge Crystallographic Data Centre and Fachinformationszentrum Karlsruhe Access Structures service.

© 2022 The Authors. Chemistry - A European Journal published by Wiley-VCH GmbH

15213765, 2023, 11, Downloaded from https://chemistry-europe.onlinelibrary.wiley.com/doi/10.1002/chem.202203501 by Koc University, Wiley Online Library on [10/05/2023]. See the Terms and Conditions (https://onlinelibrary.wiley.com/terms-and-conditions) on Wiley Online Library for rules of use; OA articles are governed by the applicable Creative Commons License

Graphical representations of the structure were created in Diamond.[43]

Vibrational spectroscopy: FT-Raman spectra were obtained using a Renishaw inVia Raman microscope equipped with a 532 nm excitation laser source. The Raman spectra of selected crystals were recorded at room temperature in the range of 4000 to 50 cm^{-1} using a Horiba LabRam HR Evolution spectrometer equipped with a He–Ne laser (633 nm) and a Synapse CCD detector.

Infrared spectra were recorded in Attenuated Total Reflectance (ATR) mode using either a Thermo Scientific iS50 FTIR spectrometer with a single reflection diamond ATR module or a PerkinElmer UATR-Two FTIR spectrometer (spectral range 4000–450 cm^{-1}).

Acknowledgements

The authors would like to thank Bodo Böhme for helpful discussions and Koç University Surface Science and Technology Center (KUYTAM) for the use of facilities for Raman and IR measurements. Open Access funding enabled and organized by Projekt DEAL.

Conflict of Interest

The authors declare no conflict of interest.

Data Availability Statement

The data that support the findings of this study are available in the supplementary material of this article.

Keywords: alkaline-earth metals · azides · crystal structures · gold · vibrational spectroscopy

[1] T. M. Klapötke, B. Krumm, M. Scherr, *J. Am. Chem. Soc.* **2009**, *131*, 72–74.
[2] R. Haiges, M. Vasiliu, D. A. Dixon, K. O. Christe, *Chem. Eur. J.* **2017**, *23*, 652–664.
[3] F. Karau, W. Schnick, *Z. Anorg. Allg. Chem.* **2007**, *633*, 223–226.
[4] W. P. Fehlhammer, W. Beck, *Z. Anorg. Allg. Chem.* **2013**, *639*, 1053–1082.
[5] U. Müller, *Z. Anorg. Allg. Chem.* **1972**, *392*, 159–166.
[6] G. E. Pringle, D. E. Noakes, *Acta Crystallogr. Sect. B* **1968**, *24*, 262–269.
[7] R. P. Manno, *Nature* **1965**, *207*, 1087–1088.
[8] W. E. Garner, L. E. Reeves, *Trans. Faraday Soc.* **1955**, *51*, 694–704.
[9] J. G. N. Thomas, F. C. Tompkins, W. E. Garner, *Proc. R. Soc. London Ser. A* **1951**, *210*, 111–125.
[10] C. S. Choi, E. Prince, *J. Chem. Phys.* **1976**, *64*, 4510–4516.
[11] O. Reckeweg, A. Simon, *Z. Naturforsch. B* **2003**, *58*, 1097–1104.
[12] F. J. Llewellyn, F. E. Whitmore, *J. Chem. Soc.* **1947**, *1947*, 881–884.
[13] E. M. Walitzi, H. Krischner, *Z. Kristallogr.* **1970**, *132*, 19–26.
[14] E. M. Walitzi, H. Krischner, *Z. Kristallogr.* **1969**, *129*, 153–156.
[15] Th. Curtius, J. Rissom, *J. Prakt. Chem.* **1898**, *58*, 261–309.
[16] G. T. Rogers, *J. Inorg. Nucl. Chem.* **1958**, *5*, 339–340.
[17] S. Afyon, P. Höhn, M. Armbrüster, A. Baranov, F. R. Wagner, M. Somer, R. Kniep, *Z. Anorg. Allg. Chem.* **2006**, *632*, 1671–1680.
[18] W. Beck, T. M. Klapötke, P. Klüfers, G. Kramer, C. M. Rienäcker, *Z. Anorg. Allg. Chem.* **2001**, *627*, 1669–1674.
[19] S. Afyon, P. Höhn, M. Somer, *Z. Anorg. Allg. Chem.* **2010**, *636*, 1301–1306.
[20] W.-K. Seok, T. M. Klapötke, *Bull. Korean Chem. Soc.* **2010**, *31*, 781–788.
[21] O. Reckeweg, H. J. Meyer, A. Simon, *Z. Anorg. Allg. Chem.* **2002**, *628*, 920–922.
[22] S. J. Clarke, F. J. DiSalvo, *Z. Kristallogr. New Cryst. Struct.* **1997**, *212*, 309–310.
[23] P. Höhn, R. Kniep, J. Maier, *Angew. Chem. Int. Ed.* **1993**, *32*, 1350–1352; *Angew. Chem.* **1993**, *105*, 1409–1410.
[24] O. Reckeweg, F. J. DiSalvo, *Z. Naturforsch. B* **2003**, *58*, 201–204.
[25] G. M. Sheldrick, *Acta Crystallogr. Sect. A Found. Crystallogr.* **2008**, *64*, 112–122.
[26] G. M. Sheldrick, *Acta Crystallogr. Sect. C Struct. Chem.* **2015**, *71*, 3–8.
[27] W. Beck, W. P. Fehlhammer, P. Pöllmann, E. Schuierer, K. Feldl, *Chem. Ber.* **1967**, *100*, 2335–2361.
[28] T. M. Klapötke, B. Krumm, J.-C. Galvez-Ruiz, H. Nöth, *Inorg. Chem.* **2005**, *44*, 9625–9627.
[29] Z. Dori, R. F. Ziolo, *Chem. Rev.* **1973**, *73*, 247–254.
[30] U. Müller, *Struct. Bond.* **1973**, *14*, 141–172.
[31] E. M. Walitzi, H. Krischner, *Z. Kristallogr.* **1970**, *131*, 25–28.
[32] S. Alvarez, *J. Chem. Soc. Dalton Trans.* **2013**, *42*, 8617–8636.
[33] J. Psilitelis, *Thesis*, Fakultät für Chemie und Pharmazie der Eberhard-Karls-Universität Tübingen (Germany), **1999**.
[34] W. Beck, T. M. Klapötke, J. Knizek, H. Nöth, T. Schütt, *Eur. J. Inorg. Chem.* **1999**, *1999*, 523–526.
[35] W. Beck, W. P. Fehlhammer, K. Feldl, T. M. Klapötke, G. Kramer, P. Mayer, H. Piotrowski, P. Pöllmann, W. Ponikwar, T. Schutt, E. Schuierer, M. Vogt, *Z. Anorg. Allg. Chem.* **2001**, *627*, 1751–1758.
[36] E. M. Walitzi, H. Krischner, *Z. Kristallogr.* **1973**, *137*, 368–379.
[37] D. N. Sathyanarayana, in *Vibrational Spectroscopy: Theory and Applications*, New Age International, **2015**.
[38] S. Seidel, M. Somer, K. Kiraz, U. Ch. Rodewald, R. Pöttgen, *Z. Anorg. Allg. Chem.* **2017**, *643*, 1831–1835.
[39] M. Jursch, *Prometheus 5.1*, Ruhr-Universität Bochum (Germany), **1997**.
[40] H. Siebert, *Z. Anorg. Allg. Chem.* **1953**, *273*, 21–27.
[41] J. Goubeau, *Ber. Bunsen-Ges. Phys. Chem* **1966**, *70*, 934.
[42] T. Steiner, *Angew. Chem. Int. Ed.* **2002**, *41*, 48–76; *Angew. Chem.* **2002**, *114*, 50–80.
[43] Crystal Impact – Dr. H. Putz and Dr. K. Brandenburg GbR, *Diamond–Crystal and Molecular Structure Visualization*, Kreuzherrenstr. 102, 53227 Bonn (Germany), **2017**.

Manuscript received: November 11, 2022
Accepted manuscript online: December 22, 2022
Version of record online: January 17, 2023

© 2022 The Authors. Chemistry - A European Journal published by Wiley-VCH GmbH

15213765, 2023, 11, Downloaded from https://chemistry-europe.onlinelibrary.wiley.com/doi/10.1002/chem.202203501 by Koc University, Wiley Online Library on [10/05/2023]. See the Terms and Conditions (https://onlinelibrary.wiley.com/terms-and-conditions) on Wiley Online Library for rules of use; OA articles are governed by the applicable Creative Commons License